

Turning calcium carbonate into a cost-effective wastewater-sorbing material by occluding waste dye

Dan-Hua Zhao · Hong-Wen Gao

Received: 3 December 2008 / Accepted: 22 January 2009 / Published online: 5 March 2009
© Springer-Verlag 2009

Abstract

Background, aim, and scope Over the years, organic pollution in the environment has aroused people's concern worldwide, especially persistent organic pollutants (POPs). Particularly in developing countries, plenty of concentrated organic wastewaters treated noneffectively are discharged into aquatic environments from chemical, textile, paper-making, and other industries to seriously threaten the surface and drinking water. The conventional wastewater treatment techniques are often helpless due to high cost with multilevel processing. Adsorption as an efficient method is often applied to the treatment of wastewater. The aim of this work is to develop an eco-friendly and cost-effective wastewater-sorbing material with weak acidic pink red B (APRB) and calcium carbonate (CaCO_3) by reusing highly concentrated dye wastewater.

Materials and methods On the basis of the chemical coprecipitation of APRB with growing CaCO_3 particles, an inclusion material was prepared. The composition of material was determined by atomic absorption spectrometry, thermogravimetric analysis, and transmission electron microscopy (TEM)-energy dispersive X-ray, and its morphology characterized by X-ray diffraction, scanning electron microscopy, TEM, and particle-size analysis. Two cationic dyes, ethyl violet (EV) and methylene blue (MB), and four POPs, phenanthrene (Phe), fluorene (Flu), biphenyl

(Bip), and biphenol A (Bpa), were used to investigate the adsorption selectivity, capacity, and mechanism of the new material, where spectrophotometry, fluorophotometry, and high-performance liquid chromatography were used for determination. An APRB-producing wastewater was reused for preparing the cost-effective wastewater-sorbing material instead of the APRB reagent and then treating cationic dye wastewaters. The remove rates of colority and chemical oxygen demand (COD) were evaluated.

Results and discussion The CO_3^{2-} -APRB- Ca^{2+} addition sequence is most favorable for the occlusion of APRB into the growing CaCO_3 particles, and the occlusion of APRB corresponded to the Langmuir isothermal adsorption with the binding constant (K) of $5.24 \times 10^4 \text{ M}^{-1}$ and the Gibbs free energy change (ΔG) of -26.9 kJ/mol . The molar ratio of Ca^{2+} to CO_3^{2-} and APRB was calculated to be 1:0.94:0.0102, i.e., approximately 92 CaCO_3 molecules occluded only one APRB. Approximately 78% of the inclusion aggregates are between 3 and 20 μm and the particles are global-like with 50–100 nm. The element mapping on Ca, S, and C indicated APRB distributed a lot of CaCO_3 , i.e., the APRB layer may be pressed between both sides of CaCO_3 layers. The molar ratio of Ca to S was calculated to 44, i.e., 88 CaCO_3 molecules carried one APRB, according to the above data. During the growing of CaCO_3 particles, APRB may be attracted into the temporary electric double layer in micelle form by the strong charge interaction between sulfonic groups of APRB and Ca^{2+} and the hydrophobic stack of long alkyl chains. Four dyes were adsorbed: reactive brilliant red X-3B and weak acid green GS as anionic dyes and EV and MB as cationic dyes. The removals of EV and MB are extremely obvious and the saturation adsorption of EV and MB just neutralized all the negative charges in the inclusion particles. The selectivity demonstrated the ion-pair attraction, i.e., the cationic adsorption capacity depends on the negative charge

Responsible editor: Hailong Wang

Electronic supplementary material The online version of this article (doi:10.1007/s11356-009-0111-y) contains supplementary material, which is available to authorized users.

D.-H. Zhao · H.-W. Gao (✉)
State Key Laboratory of Pollution Control and Resource Reuse,
College of Environmental Science and Engineering,
Tongji University,
Shanghai 200092, China
e-mail: hwgao@tongji.edu.cn

number of the inclusion material. By fitting the Langmuir isotherm model, the monolayer adsorptions of EV and MB were confirmed. Their K values were calculated to be 2.4×10^6 and $7.3 \times 10^5 \text{ M}^{-1}$, and ΔG was calculated to be 36.4 and -33.4 kJ/mol . The adsorption of four POPs on the material obeyed the lipid–water partition law, and their partition coefficients (K_{pw}) were calculated to be 9,342 L/kg for Phe, 7,301 L/kg for Flu, 1,226 L/kg for Bip, and 870 L/kg for Bpa. The K_{pw} is the direct ratio to their lipid–water partition coefficients (K_{ow}) with 0.314 of slope. Besides this, a cost-effective $\text{CaCO}_3/\text{APRB}$ inclusion material was prepared with an APRB-producing wastewater instead of APRB reagent, and it was used in the treatment of two practical cationic dye wastewaters (samples A and B). The colority and COD in sample B are 18 and 13 times high as those of sample A. The decolorization of sample A is over 96%, and the removal of COD is between 70% and 80% when more than 0.3% adsorbent was added. However, those of sample B are over 98% and 88% in the presence of over 1% adsorbent. The adsorbent added in sample B, which was only two to three times as high as that in sample A, brought a similar removal rate of colority and COD. The inclusion material is more efficient for treatment of a highly concentrated dye wastewater because it may adsorb the most cationic dye up to saturation.

Conclusions A cost-effective onion-like inclusion material was synthesized with the composition ratio 90 ± 2 of CaCO_3 to APRB, and it carried a lot of negative charges and lipophilic groups. It has a high adsorption capacity and rapid saturation for cationic dye and POPs. The adsorption of cationic dyes corresponded to the Langmuir isothermal model and that of POPs to the lipid–water partition law. The adsorbent is suitable for treatment of concentrated cationic dye and POPs wastewater in neutral media. The addition quantity of the calcium carbonate–APRB adsorbent was suggested below: only 3–5 kg per ton of wastewater (<1,000 colority or <2 mg/L POPs) and 20–30 kg per ton of highly concentrated wastewater (>20,000 colority or >50 mg/L POPs).

Recommendations and perspectives The skeleton reactants are low-cost, easily available, and harmless to the ecological environment; additionally, the APRB reactant can reuse APRB-producing wastewater. The dye-contaminated sludge can potentially be reused as the color additive in building material and rubber and plastics industries. However, the APRB and dye contaminant would be released from the sludge when exposed to an acidic media (pH <4) for long time. This work has developed a simple, eco-friendly and practical method for the production of a cost-effective wastewater-sorbing material.

Keywords Adsorption · Calcium carbonate · Chemical coprecipitation · Inclusion material · Wastewater treatment · Weak acidic pink red B

1 Background, aim, and scope

Environmental pollution by dyes and persistent organic pollutants (POPs) is a threatening problem for ecology and public health in affected areas. Over 100,000 dyes have been synthesized worldwide and more than 700,000 tones is produced annually, over 5% of which is discharged into aquatic environments (McMullan et al. 2001; Gong et al. 2005). Especially in developing countries, plenty of dye wastewater is not treated effectively (Chen et al. 2002). As an example, over 100 dye plants and users are distributed in the economically developed Yangtze Delta Area of China, where Taihu Lake is the major drinking water source. In recent years, discharge of plenty of dye wastewater has seriously limited the local economic development and seriously affected people's health (Yang et al. 2008; Pandit and Basu 2004; Guo 2007). POPs, such as polycyclic aromatic hydrocarbons (PAHs), are commonly detected at elevated concentrations in stormwater runoff and wastewater streams. POPs originate from predominantly anthropogenic sources, such as complete combustion of fuels and discharges from industrial and wastewater treatment plants. Once in the environment, dyes and POPs are recalcitrant due to their high chroma or low solubility and resistance to biodegradation. The majority of the dyes and POPs are toxic and even carcinogenic and cause damage not only to aquatic life but also to humans (Schenker et al. 2007; Fu and Viraraghavan 2001; Monson et al. 1995; Arfsten et al. 1996). Most aromatic dyes and POPs are stable and resistant to temperature, heat, and light. Azo dyes are resistant to breakdown in microbe media (Talarposhti et al. 2001). There are many methods used for treatment of organic wastewater, such as adsorption, electrocoagulation, electro-oxidation, biological degradation, advanced oxidation processes, chemical coagulation, flocculation and filtration, etc. (Ugurlu and Kula. 2007; Xing et al. 2008; Banate et al. 1996; Atkinson et al. 1998; Crini 2006). Currently, there is no such economical and easy solution to the treatment of highly concentrated organic wastewater. Adsorption, as one of the simple and effective methods, is often applied to the treatment of dye and POPs wastewaters. Especially, various adsorbents, e.g., activated carbon, wood sawdust, bentonite, waste leave, and sludge, are utilized (Gonzalez et al. 2008; Laasri et al. 2007, Gomez et al. 2007; Crini and Badot 2008). However, low adsorbing capacity, lack of selectivity, slow adsorption equilibrium, and difficult reproduction (Robinson et al. 2001, Vijayaraghavan and Yun 2008) often restrict the extensive use of adsorbents. The purpose of this work is to develop an effective and low-cost wastewater-sorbing material by using CaCO_3 with occlusion of weak acidic pink red B (APRB) from wastewater, with the aim to reuse and recycle organic wastewater.

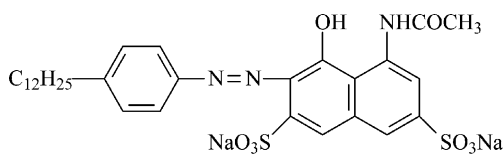
2 Materials and methods

2.1 Instruments and apparatus

A Model S-4100 Photodiode Array Spectrophotometer (Scinco Instruments, Korea) with Labpro plus software (Firmware Version 060105) was used to determine APRB. A Model Analyst 400 Atomic Absorption Spectrophotometer (Perkin-Elmer Instruments, USA) was used to determine calcium content in the inclusion material. A Model TG16-WS centrifugal machine (Hunan Xiangyi Instruments, China) was used to separate the inclusion material from the solution. A Model LS230 Particle Size Analyzer (Beckman Coulter, USA) with a Model LFC-101 Laser Channel (Ankersmid, Holland) was used to measure the size distribution of the inclusion material with the LS v3.29 operation software installed. A Model D/max2550VB3+/PC X-ray diffractometer (XRD) (Rigaku Intern., Japan) was used for identifying the crystal structure and size. A Model Quanta 200 FEG scanning electron microscopy (SEM) (FEI, USA) was used to investigate the size and structure of the inclusion material. Elemental analysis and element mapping on carbon, oxygen, sodium, sulfur, and calcium were conducted with a JEM-2100 (Japan Electron Kabushiki Kaisha) transmission electronic microscope equipped with an energy dispersive X-ray spectroscopy (EDX) of inca oxford (England, Oxford). A high-resolution transmission electronic microscopy (HRTEM) (Model Tecnai G2 F20 S-Twin, FEI, USA) (120 kV, 2.4 Å resolution) was used to measure the distribution of CaCO₃ and APRB in the particle fragments.

2.2 Preparation and characterization of the inclusion materials

A commercial APRB reagent (CAS No.15792-43-5) (Fig. 1) was purified with DMF and chloroform before preparation of the inclusion material. Two hundred milliliters of 1.0 mmol/l APRB was added into one 2,000-ml beaker with 600 ml of ethanol; 200 ml of 100 mmol/l CaCl₂ was then added and mixed thoroughly by stirring before 200 ml of 50 mmol/l Na₂CO₃ was added slowly. The reaction liquid was stewed for precipitating the suspending substances, and then the precipitate was washed with



APRB (C.I. 18073)

Fig. 1 The chemical structure of APRB

2,000 ml of deionized water three times. The final suspending substance liquid with concentrated CaCO₃/APRB inclusion material was used as the product. In order to yield a practical and cost-effective sorbent, APRB wastewater was tested as a reactant in this work. An APRB-producing wastewater [pH 8.6, 23,000 mg/l chemical oxygen demand (COD) and 0.074% APRB] was collected from a chemical plant. With the same method, the CaCO₃/APRB inclusion material was prepared with the above APRB wastewater instead of APRB reagent. The APRB concentration in the liquids was determined at 518 nm by spectrophotometry and the suspending substances produced in the reaction were centrifuged at 5,000 rpm for 5 min. By dissolving the CaCO₃/APRB inclusion material in 0.1 mol/L ethylenediaminetetraacetic acid (EDTA), Ca content was determined by inductively coupled plasma-optical emission spectrometry, APRB by spectrophotometry. The CO₃²⁻ in the adsorbent was determined by the carbon dioxide quantity released in 1 mol/L hydrochloric acid (GB/T 218-1996 1996). The thermogravimetric analysis (TGA), XRD, SEM, and transmission electron microscopy of both the CaCO₃-only and CaCO₃/APRB inclusion material powders were measured for determination of the composition ratio and analysis of microstructure of the materials. The size distribution and surface electricity of the suspending adsorbent in liquid were measured by a laser particle-size analyzer and a ζ-potential detecting-device, respectively.

2.3 Adsorption of dyes and POPs

Four dyes, reactive brilliant red X-3B (CAS No. 12226-03-8), weak acid green GS (CAS No. 6408-57-7), ethyl violet (EV) (CAS No. 2390-59-2), and methylene blue (MB) (CAS No. 7220-79-3), and four POPs, Phe, Flu, Bip, and Bpa, were prepared for investigating the adsorption selectivity, performance, and mechanism of the CaCO₃/APRB inclusion material, where the concentration of dyes was determined by spectrophotometry and that of POPs by fluorophotometry and high-performance liquid chromatography. Meanwhile, the adsorption ability of the inclusion material was compared with powder-activated carbon with 800–1,000 m²/g of specific surface area (SSA).

2.4 Treatment of dye wastewaters with the inclusion material

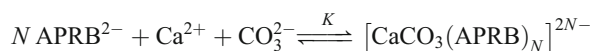
Two cationic dye wastewaters were sampled from Jinjiang Dye Factory (Hangzhou, China), and they were treated with the inclusion material prepared from the APRB wastewater. The colority and COD of wastewaters were determined with spectrophotometer and a rapid COD analyzer, respectively.

3 Results and discussion

3.1 Synthesis and composition of the inclusion material

Chemical coprecipitation as a classical method is often applied to the enrichment of a trace substance (Geets et al. 2006; Sathe et al. 2006; Mustafa et al. 2008; Baumann and Hatmaker 1961) and synthesis of a functional material (Wisian-Neilson 2003; Schur et al. 2003). From change of the absorption spectra of the CaCO₃-only liquid, the gradient increased with increase in ethanol (supporting information online Fig. S1A). It indicates that ethanol may slow down the growth of CaCO₃ and thin the particles (Gao 1992). When ethanol was over 40%, the particle size was too small to settle down. The occlusion of APRB in CaCO₃ particles remained maximal when ethanol was over 20% (Fig. S1B). From the effect of three addition sequences (Fig. S1C), the third sequence, CO₃²⁻-Ca²⁺-APRB, gives the least capture amount of APRB. The reason is that CaCO₃ particles were formed before the addition of APRB. Thus, APRB was adsorbed only into the colloidal electric double layers on the outside surface of CaCO₃ particles (Baumann and Hatmaker 1961). The particles prepared by this way were the CaCO₃/PRB surface-modifying material. The second sequence, Ca²⁺-APRB-CO₃²⁻, obtained greater occlusion of APRB than the third sequence. First of all, Ca²⁺ reacted with APRB to form the Ca-APRB complex, which is ineffective for the adsorption of cationic dye. Thus, the following CO₃²⁻ must competitively replace the APRB binding to Ca²⁺ to form the CaCO₃/APRB inclusion material. Therefore, it is possible that the sediment formed in the second addition sequence contained a lot of the ineffective Ca-APRB complex. The first addition sequence, CO₃²⁻-APRB-Ca²⁺, is most favorable for the occlusion of APRB into the growing CaCO₃ particles in layer-on-layer. As a result, such a sequence was used to prepare the object material. From the effect of Ca²⁺ concentration on the formation of CaCO₃ particles (Fig. S1D), the particle size decreased with an increase of Ca²⁺, but the sediment amount increased. In addition, the ineffective Ca-APRB compound with 5.2 × 10⁻⁸ of the solubility product constant (*K*_{sp}) (Fig. S2) would be formed if the initial Ca²⁺ is too excessive. The initial mole ratio of Ca²⁺ to CO₃²⁻ was selected at 2.

The complexation among APRB (R), Ca²⁺, and CO₃²⁻ (M) may be expressed as:



Initiation	$c_{0,R}$	$c_{0,M}$	0
Equilibrium	c_R	$c_{M \rightarrow 0}$	$c_{0,M}$

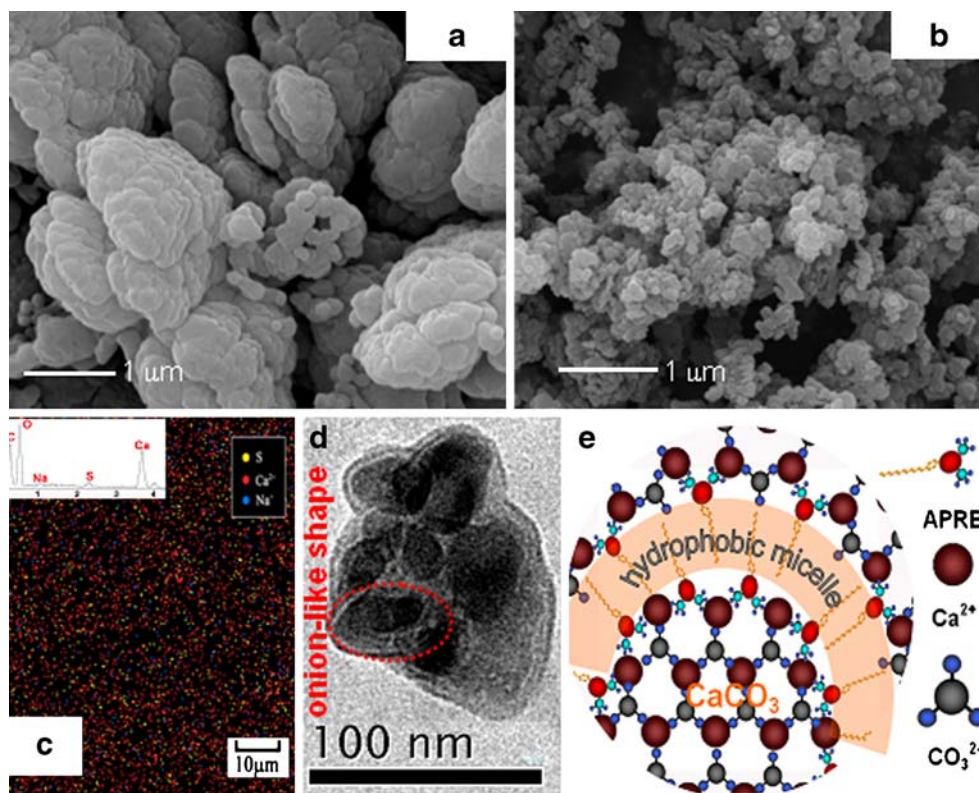
The symbol *N* is the saturating number of APRB and *K* is the adsorption constant. $c_{0,R}$ and $c_{0,M}$ are the initial molar concentrations of APRB and CO₃²⁻, while c_R and c_M represent their equilibrium molarity. c_M approaches zero when the molarity of Ca²⁺ is higher than that of CO₃²⁻. The mole number (γ) of APRB including into CaCO₃ particles is calculated by the relation $\gamma = \eta c_{0,R} / c_{0,M}$, where the effective fraction (*h*) of APRB is calculated by $\eta = 1 - c_R / c_{0,R}$. With increasing APRB molarity, γ approaches *N*. From the effect of initial APRB molarity ($c_{0,R}$) (Fig. S3A), the occlusion of APRB approached a constant maximum at $N=0.018$ when $c_{0,R}/c_{0,M}$ is more than 0.025. It indicated that 56 CaCO₃ molecules can occlude a maximum of one APRB molecule. The Langmuir isothermal model was used to fit the experimental data (Fig. S3B) and the binding constants (*N*; *K*; and the Gibbs free energy change, ΔG) were calculated to be $N=0.02$, $K=5.24 \times 10^4 \text{ M}^{-1}$ and $\Delta G=-26.9 \text{ kJ/mol}$. Therefore, the inclusion of APRB in CaCO₃ particles corresponded to the spontaneous chemical adsorption. APRB may be attracted into the temporary electric double layer (TEDL) in micelle by the affinity of sulfonic groups with Ca²⁺ and the hydrophobic stack of long alkyl chains. However, η decreased with an increase of $c_{0,R}/c_{0,M}$ (Fig. S3A), i.e., excess APRB would react with excess Ca²⁺ to form the ineffective material. Therefore, $c_{0,R}/c_{0,M}$ is suitably selected between 0.015 and 0.020. The effect of pH on the occlusion of APRB was determined (Fig. S4). The CaCO₃ particle sediment was dissolved when pH was less than 3. γ remains at an almost constant maximum when pH is more than 4.5. The preparation of the inclusion material is selected in neutral media in this work. According to the above optimal experimental conditions, a suspending solid (SS) liquid of the CaCO₃/APRB inclusion material was synthesized. After the SS liquid rested for 2 h and the supernatant was removed, the solid content of the final concentrated SS liquid was determined to be 23%. Unlike the conventional flocculate, the solid particles are non-flocculated. After the SS was dissolved in an EDTA solution, Ca²⁺ was determined to be 10.1 ± 0.1 mmol per milligram of solid, CO₃²⁻ 9.5 ± 0.1 mmol/mg, and APRB 0.103 ± 0.001 mmol/mg. Thus, the molar ratio of Ca²⁺ to CO₃²⁻ and APRB in the inclusion material was calculated to be 1:0.94:0.0102. Therefore, the addition of APRB has not affected the formation of CaCO₃. No covalent bond was formed between APRB and CaCO₃, i.e., APRB was occluded via the strong charge interaction (Cong et al. 2007). Approximately 92 CaCO₃ molecules occluded only one APRB in the work material, which is only half of the saturation binding number of APRB above. It is attributed to the fact that the coexistence of some unknown organic substances in the APRB wastewater, e.g., excessive reactants, by-products, and electrolytes, may interfere with the layer-on-layer inclusion of APRB.

3.2 Characterization of the particles

From TGA of three kinds of materials, e.g., APRB-only, CaCO₃-only, and CaCO₃/APRB inclusion particles (Fig. S5), APRB could undergo a thermal decomposition at below 600°C, and the weight loss was 70%. The weight loss of APRB powder was 26% around 280°C and 27% around 430°C. The former may be caused by the volatilization of alkyl chain -C₁₂H₂₅ and the latter by the decomposition of azo naphthol amide. Above 600°C, the two sulfonic groups of APRB could be transformed into sodium sulfate. Above 760°C, the obvious weight loss of CaCO₃ occurred owing to the thermal decomposing into CaO. The weight loss of APRB in the CaCO₃ inclusion material was 5% between 200 and 600°C by correcting with the CaCO₃-only material. Therefore, the mass percentage of APRB was calculated to be 7% in the CaCO₃/APRB inclusion material, i.e., the molar ratio of APRB to CaCO₃ is approximately 1:90. The self-aggregate of CaCO₃-only particles in aqueous liquid is highly nonuniform, and most of them are between 3 and 40 μm (Fig. S6A). However, approximately 78% of the inclusion aggregates are between 3 and 20 μm (Fig. S6B), and the big particles over 20 μm decreased obviously. Therefore, the participation of APRB affected the self-aggregation of CaCO₃ particles. From the SEM images (Fig. 2a), the

CaCO₃-only particles are nonuniform like the mushrooms of varying sizes, most of which are more than 2 μm. This is attributed to the dense packing of CaCO₃ layers. On the contrary, the CaCO₃/APRB inclusion particles are global-like with 50–100 nm of size and the mutual adhesion of nanoparticles formed the shapeless aggregates with the clear particle borderline (Fig. 2b). Therefore, the participation of APRB inhibited the self-stack of CaCO₃ molecules but did not alter the formation of CaCO₃ from the XRD data (Fig. S7). The active species of the inclusion material not only exposed enough (see Fig. 2b) but the aggregates also settled down easily. Thus, the inclusion material may be suitable as an adsorbent of cationic organic substances. The elemental analysis and element mapping on Ca, O, Na, S, and C were performed by EDX (Fig. 2c). The S indicating APRB (yellow points) always distributes around a lot of Ca points (red). The molar ratio of Ca to S was calculated to 44, i.e., 88 CaCO₃ molecules carried one APRB molecule in the work material. Besides this, the Na points (blue) (see Fig. 2c) indicated that Na⁺ may be attracted in the solid inclusion particles for maintaining the charge equilibrium together with Ca²⁺. From almost the same *N* values of APRB obtained by various detection methods above, approximately 45 mol of CaCO₃ carried only 1 mol of negative charges in the work material. From the HRTEM image of a fragment of CaCO₃/APRB

Fig. 2 SEM images of CaCO₃-only (a) and CaCO₃/APRB inclusion material (b). c The element mapping of the inclusion material with elemental analysis measured by EDX, d HRTEM of a CaCO₃/APRB aggregate, and e cartoon illustration of APRB including into CaCO₃



inclusion particles (Fig. 2d), the APRB layer is fixed as a sandwich between striated CaCO_3 layers. The onion-like inclusion particles were formed and they further aggregated together.

From the above results, APRB was adsorbed and occluded in CaCO_3 particles, and the formation process of negatively charged CaCO_3 /APRB coprecipitate is illustrated in Fig. 2e. APRB with a long alkyl chain formed micelle aggregates in aqueous phase. During the slow growing of CaCO_3 particles, APRB was adsorbed on the TEDL and bound with the inner CaCO_3 by complexation. The aggregation of APRB formed a micelle layer via the hydrophobic stack of the long alkyl chains. Immediately, Ca^{2+} bound on the polar heads of the outer APRB layer, but then, CO_3^{2-} captured the Ca^{2+} to form an inorganic CaCO_3 encircling shell because K_{sp} of CaCO_3 is much less than that of the Ca-APRB complex. The inclusion material carried a lot of negative charges, confirmed by measurement of the z-potential of the materials' liquids: -21.0 mv for the inclusion material and only -11.5 mv for CaCO_3 -only. Without doubt, the inclusion material can be used as an efficient adsorbent to treat organic wastewater containing cationic organic substances, e.g., cationic dyes.

3.3 Adsorption of cationic dyes and POPs

The dye-inclusion materials are often synthesized for solar cell and functionalized membrane (Zhang et al. 2008; Bach et al. 1998; Takahashi et al. 2006; Sourisseau 2004). Nevertheless, no inclusion material was used as adsorbent applied in pollution control. The adsorptions of four dyes on the CaCO_3 /APRB inclusion material were carried out: reactive brilliant red X-3B and weak acid green GS as anionic dyes and EV and MB as cationic dyes. At the same time, the CaCO_3 -only and CaCO_3 /APRB surface-modifying materials were used to compare the adsorption performance according to the same operation instead of the inclusion material. From Fig. 3, both anionic dyes A and B were hardly adsorbed by the two materials. On the contrary, the removals of EV and MB (C and D) are extremely obvious when treated with the inclusion material while the surface-modifying material is effective to adsorb both dyes. The CaCO_3 -only material has no obvious removal effect for all the dyes. Therefore, such a sorption selectivity clarified that the interactions of cationic organic compounds with the material are mainly due to the charge attraction. Moreover, the inclusion material contains more negative charges than the surface-modifying material. This again confirms that the CaCO_3 /APRB inclusion particle will form a negatively electronic aggregate in aqueous phase.

Studies on the adsorption mechanism are a prerequisite to understand the adsorbate-adsorbent interaction. The adsorptions of EV and MB on the CaCO_3 /APRB inclusion

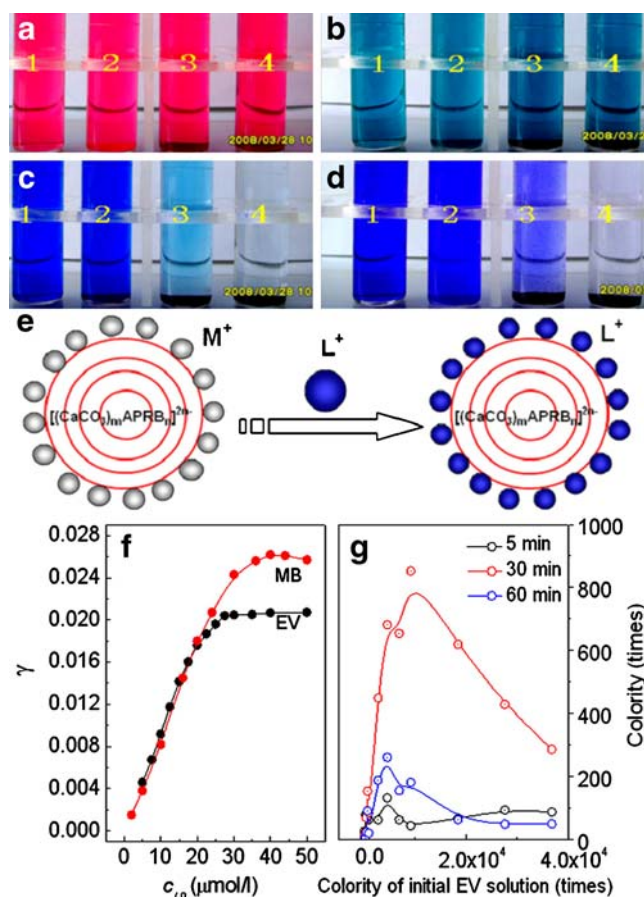


Fig. 3 Images of the dye solutions containing reactive brilliant red X-3B (a), weak acid green GS (b), EV (c), and MB (d); all are $100 \mu\text{M}$. 1 Dye-only. From 2 to 4 treated with the CaCO_3 only, CaCO_3 /APRB surface-modifying, and CaCO_3 /APRB inclusion materials. e Cartoon illustration of adsorption of cationic dye L (EV or MB) on the inclusion material. f Plots γ vs. c_{L0} of EV and MB, and g variation of colority of the EV solutions treated with the inclusion material at 5 min and activated carbon at 30 and 60 min

material were investigated in detail. From plots γ vs. c_{L0} (see Fig. 3f), γ values of EV and MB remain at constant maximums: 0.020 and 0.025 when their initial concentrations are more than 30 mmol/L, i.e., 40–50 mol of CaCO_3 can capture only 1 mol of EV or MB at saturation. By contrasting N of APRB including in CaCO_3 , the saturation adsorption of EV or MB just neutralized all the negative charges of the onion-like inclusion particles, i.e., the reaction occurred: $[(\text{CaCO}_3)_m(\text{APRB})_n]^{2n-} + 2n\text{L}^+ = \text{L}_{2n}[(\text{CaCO}_3)_m(\text{APRB})_n]^-$ (L: EV or MB, $m \approx 90n$) illustrated in Fig. 3e. It again gives evidence of the electronic charge pairing interaction. As a deduction, APRB is the unique active species occluded in the CaCO_3 skeleton. Furthermore, the APRB included in the CaCO_3 particle inside is able to play the charge attraction role, i.e., the cationic adsorption capacity of the inclusion material depends on the

number of charges. The adsorption capacity of the adsorbent has no direct correlation with the SSA of particles. Therefore, all the negative charges of the inclusion particle were neutralized electrically in a saturation adsorption solution. By fitting the Langmuir isotherm model, the monolayer adsorptions of EV and MB on the inclusion material were confirmed. Their K values were calculated to be 2.4×10^6 and $7.3 \times 10^5 \text{ M}^{-1}$, respectively, and their ΔG -36.4 and -33.4 kJ/mol . Therefore, the interaction of cationic dye with the inclusion material belongs to the spontaneous chemical adsorption.

In addition, the natural settling of the particles adsorbing MB was investigated for the requirement of the practical wastewater treatment. The results indicate that most of the particles were separated completely at only 1 h in an $h/d=1$ columnar pool (h , pool height, and d , pool diameter) and 3 h in an $h/d=3$ pool (Fig. S8). Moreover, the water ratio of the final settlement sludge was only 75% (w/w), which is much less than that generated with the conventional ferriferrous or aluminiferous flocculation agents. The sorption of EV on the $\text{CaCO}_3/\text{APRB}$ inclusion material with only $0.54 \text{ m}^2/\text{g}$ of SSA was compared with the classical activated carbon powder with $800\text{--}1,000 \text{ m}^2/\text{g}$ of SSA. From Fig. 3g, the adsorption of EV on the $\text{CaCO}_3/\text{APRB}$ inclusion material was complete in only 5 min. However, the colority of EV treated by activated carbon becomes minimal only when a strong mixing is performed over 60 min. In order to overcome the capillary effect, activated carbon must be used under a long-time strong mixing (Bacaoui et al. 2002; Gupta et al. 2006). Though the final removal rates of EV are similar using both materials, the inclusion material is much quicker than activated carbon in the adsorption of EV. Without doubt, the inclusion material has quite a different mechanism from that of activated carbon. The former depends mainly on the carrying electric

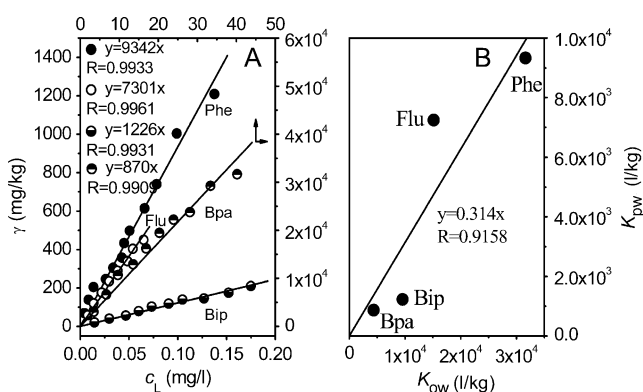


Fig. 4 a Plots γ vs c_L of POPs where 0.03% (w/w) of the $\text{CaCO}_3/\text{APRB}$ inclusion adsorbent were added in 50–500 $\mu\text{g/L}$ Phe, 25–200 $\mu\text{g/L}$ Flu, 0.05% in 25–300 $\mu\text{g/L}$ Bip, and 5–48 mg/L Bpa, and b the correlation between K_{pw} and K_{ow}

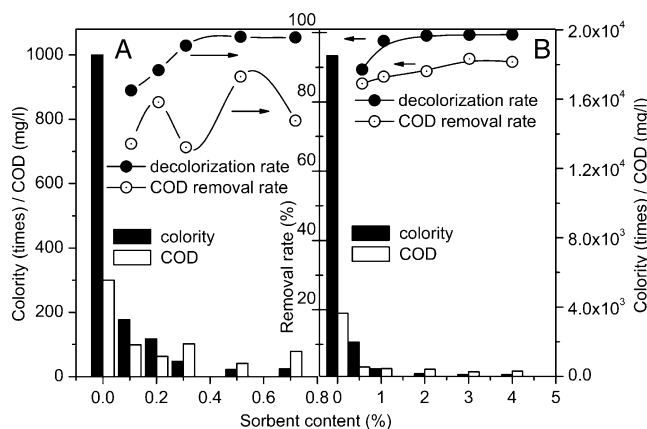


Fig. 5 The decolorization rate and COD removal rate of two dye wastewaters. a Treatment of low-colority wastewater with the $\text{CaCO}_3/\text{APRB}$ inclusion material added from 0.1 to 0.7% (w/w); b treatment of high-colority wastewater with the adsorbent added from 0.5% to 4.0% (w/w)

charge quantity, but the latter depends on the SSA. As a result, use of the $\text{CaCO}_3/\text{APRB}$ inclusion material in treatment of a cationic dye wastewater has the advantages of, e.g., high adsorption capacity, fast adsorption equilibrium, quick settlement, and low sludge volume. The effects of pH and ionic strength on the adsorption of EV were investigated with the $\text{CaCO}_3/\text{APRB}$ inclusion material (Fig. S9). γ of EV increased with increasing pH from 3 to 4 and remained almost constant at pH over 4. This is due to the dissolution of CaCO_3 particles. γ of EV decreased rapidly with increasing electrolyte from 0 to 1.0 M. This indicated that the adsorption capacity of $\text{CaCO}_3/\text{APRB}$ inclusion material was influenced by ionic strength. Therefore, the adsorbent is more suitable for treatment of weakly acidic and neutral wastewater with less than 5,000 mg/L of salinity.

Besides, APRB owns a long alkyl chain, $-\text{C}_{12}\text{H}_{25}$ group (see Fig. 1) and the APRB molecules adsorbing on the outside surface of the material will form a hydrophobic shell to adsorb lipophilic organic substances, e.g., strongly cancerogenic POPs (Arnot and Mackay 2008; Chung et al. 2007). In this work, three PAHs, phenanthrene (Phe), fluorene (Flu), biphenyl (Bip) and biphenol A (Bpa), were used as POPs for examining the adsorption capacity of the inclusion material. γ of POPs were calculated as shown in Fig. 4a. Different from the cationic dye (see Fig. 3f), the adsorption of POPs has no equilibrium tendency. Plots γ vs c_L demonstrated a good linear relationship. Therefore, the adsorption of POPs on the inclusion material accorded with the lipid–water partition law and the hydrophobic interaction occurred between the long alkyl chain of APRB and POPs. Their partition coefficients (K_{pw}) in the $\text{CaCO}_3/\text{APRB}$ inclusion material were calculated to be 9,342 L/kg for Phe, 7,301 L/kg for Flu, 1,226 L/kg for Bip, and 870 L/kg for Bpa (Fig. 4b). The K_{pw} is the almost direct ratio to the

corresponding K_{ow} (Dong and Chang 2000; Qu et al. 2007) with 0.314 of slope, i.e., 3 g of the inclusion material played the role equivalent to 1 g of octanol in the removal of POPs. The effect of time and temperature on the adsorption of Flu indicated that the saturation adsorption is complete in 2 min (Fig. S10) and that temperature has no obvious effect between 10 and 40°C. In order to evaluate the competitive adsorption of various POPs, a uniform solution mixed with Phe, Flu, and Bip (each 0.100 mg/L) and Bap (2.00 mg/L) was treated with the CaCO₃/APRB inclusion material. From the removal of POPs (Fig. S11B), the removal rates of Phe, Flu, and Bip increased synchronously with an increase in the material percentage. No Bpa was removed when the material was less than 0.1%. By comparison with the single POP (Fig. S11A), the removal rates of both Flu and Phe decreased by 30%, that of Bip changed little, and that of Bpa decreased from 30% down to 0. This indicated that PAHs were adsorbed on the adsorbent prior to Bpa.

3.4 Treatment of dye wastewater

Recycle and reuse of waste has attracted more and more attention (Liu et al. 2008; Gilbert et al. 1976; Tal 2006; Ng et al. 2007). The CaCO₃/APRB inclusion material was prepared with an APRB-producing wastewater instead of APRB reagent, and it was applied to the treatment of two typical cationic dye wastewaters. From change of the column height (Fig. 5), the colority of two wastewaters decreased obviously with an increase in the adsorbent percentage. The decolorization of sample A is over 96% (see Fig. 5a) and the removal rate of COD is between 70% and 80% from curve 4 when more than 0.3% of the material is added. Similarly, the removal rates of colority and COD of sample B are over 98% (Fig. 5b) and 88% from curve 4 when more than 1% of the material was added. The colority and COD of sample B are 18 and 13 times as high as those of sample A. Interestingly, when the adsorbent in sample B was only two to three times as high as that in sample A, it caused similar removal rates of colority and COD. This is attributed to the fact that the material may adsorb the most cationic dye molecules up to saturation in a more concentrated dye wastewater. On the contrary, the adsorbent has not adsorbed enough cationic dye molecules in a diluted dye wastewater. The inclusion material is more efficient when treating a concentrated cationic dye wastewater. From a wastewater stream, the addition quantity of the calcium carbonate–APRB inclusion material was suggested: only 3–5 kg per ton of wastewater (<1,000 colority or <2 mg/L POPs) and 20–30 kg per ton of concentrated wastewater (>20,000 colority or >50 mg/L POPs). As a multipurpose reuse prospect, the contaminated adsorbent, i.e., sludge produced during a dye wastewater treatment, has potential as the raw material of caustic lime-

making or as a color additive used in building materials and rubber and plastics industries. However, the latter reuse may cause the release of APRB and dye contaminant from the sludge when exposed to an acidic media (pH <4) for a long time.

4 Conclusions

A new, highly-effective adsorbent was developed by the coprecipitation of APRB with CaCO₃. The composition ratio of adsorbent is 90±2 of CaCO₃ to APRB. As the aggregate of the CaCO₃–APRB nanosized particles, it carried a lot of negative charges and lipophilic groups. The removals of EV, MB, four kinds of POPs, and treatment of the practical dye wastewaters indicated that the inclusion material has a very high adsorption capacity for cationic dye and POPs. The adsorption of cationic dyes corresponded to the Langmuir isothermal model via the charge attraction and that of POPs to the lipid–water partition law via hydrophobic stacking. The skeleton reactants are low-cost, easily available, and harmless to the environment; additionally, the APRB reactant may reuse a concentrated APRB-producing wastewater instead. This work has developed a simple, eco-friendly, and practical method for large-scale production of an efficient and low-cost inclusion material. It will be very significant for environmental conservation and the protection of the health of people.

Acknowledgements We thank the State Key Laboratory Foundation of Science and Technology Ministry of China (Grant No. PCRRK08003) and the National Key Technology R&D Program of China (No. 2008BAJ08B13) for financially supporting this work.

References

- Atkinson BW, Bux F, Kusan HC (1998) Considerations for application of biosorption technology to remediate metal-contaminated industrial effluents. *Water SA* 24:129–135
- Arfsten DP, Schaeffer DJ, Mulveny DC (1996) The effects of near ultraviolet radiation on the toxic effects of polycyclic aromatic hydrocarbons in animals and plants: a review. *Ecotoxicol Environ Saf* 33:1–24
- Arnot JA, Mackay D (2008) Policies for chemical hazard and risk priority setting: Can persistence, bioaccumulation, toxicity, and quantity information be combined? *Environ Sci Technol* 42:4648–4654
- Bacaoui A, Dahbi A, Yaacoubi A, Bennouna C, Maldonado-Hódar FJ, Rivera-Utrilla J, Carrasco-Marfán F, Moreno-Castilla C (2002) Experimental design to optimize preparation of activated carbons for use in water treatment. *Environ Sci Technol* 36:3844–3849
- Bach U, Lupo D, Compte P, Moser JE, Weissortel F, Salbeck J, Spreitzer H, Grmizel M (1998) Solid-state dye-sensitized mesoporous TiO₂ solar cells with high photon-to-electron conversion efficiencies. *Nature* 395:583

- Banate IM, Nigam P, Singh D, Marchant R (1996) Microbial decolorization of textile-dyecontaining effluents: a review. *Bioresour Technol* 58:217–225
- Baumann ML, Hatmaker AL (1961) Ultramicro- and micro-determination of chloride by argentimetric titration with the indicator dichlorofluorescein. *Clin Chem* 7:256–263
- Chen CC, Zhao W, Li J, Zhao J, Hidaka H, Serpone N (2002) Formation and identification of intermediates in the visible-light-assisted photodegradation of sulforhodamine-B dye in aqueous TiO₂ dispersion. *Environ Sci Technol* 36:3604–3611
- Cong HP, Yu SH (2007) Hybrid ZnO-dye hollow spheres with new optical properties from a self-assembly process based on Evans blue dye and cetyltrimethylammonium bromide. *Adv Funct Mater* 17:1814–1820
- Crini G (2006) Non-conventional low-cost adsorbents for dye removal: a review. *Bioresour Technol* 97:1061–1085
- Crini G, Badot PM (2008) Application of chitosan, a natural aminopolysaccharide, for dye removal from aqueous solutions by adsorption process using batch studies: a review of recent literature. *Prog Polym Sci* 33:399–447
- Chung MK, Hu R, Wong MH, Cheung KC (2007) Comparative toxicity of hydrophobic contaminants to microalgae and higher plants. *Ecotoxicology* 16:393–402
- Dong RA, Chang SM (2000) Determination of distribution coefficients of priority polycyclic aromatic hydrocarbons using solid-phase microextraction. *Anal Chem* 72:3647–3652
- Fu Y, Viraraghavan T (2001) Fungal decolorization of wastewaters: a review. *Bioresour Technol* 79:251–262
- Gao HW (1992) Determination of Ca²⁺ in natural water by dual-wavelength spectrophotometry. *Shanghai Environ Sci* 11:28–29
- GB/T 218-1996 (1996) Determination of carbon dioxide content—the mineral carbonates associated with coal (China)
- Geets J, Vanbroekhoven K, Borremans B, Vangronsveld J, Diels L, van der Lelie D (2006) Column experiments to assess the effects of electron donors on the efficiency of in situ precipitation of Zn, Cd, Co and Ni in contaminated groundwater applying the biological sulfate removal technology. *Environ Sci Pollut Res* 13:362–378
- Gilbert RG, Rice RC, Bouwer H, Gerba CP, Wallis C, Melnick JL (1976) Wastewater renovation and reuse: virus removal by soil filtration. *Science* 192:1004–1005
- Gong RM, Li M, Yang C, Sun YZ, Chen J (2005) Removal of cationic dyes from aqueous solution by adsorption on peanut hull. *J Hazard Mater B* 121:247–250
- Gomez V, Larrechi MS, Callao MP (2007) Kinetic and adsorption study of acid dye removal using activated carbon. *Chemosphere* 69:1151–1158
- Gonzalez M, Mingorance MD, Sanchez L, Pena A (2008) Pesticide adsorption on a calcareous soil modified with sewage sludge and quaternary alkyl-ammonium cationic surfactants. *Environ Sci Pollut Res* 15:8–14
- Guo L (2007) Doing battle with the green monster of Taihu lake. *Science* 317:1166
- Gupta VK, Mittal A, Jain R, Mathur M, Sikarwar S (2006) Adsorption of Safranin-T from wastewater using waste materials- activated carbon and activated rice husks. *J Colloid Interf Sci* 303:80–86
- Laasri L, Elamrani MK, Cherkaoui O (2007) Removal of two cationic dyes from a textile effluent by filtration-adsorption on wood sawdust. *Environ Sci Pollut Res* 14:237–240
- Liu WZ, Huang F, Liao YQ, Zhang J, Ren GQ, Zhuang ZY, Zhen JS, Liu Z, Wang C (2008) Treatment of CrVI-containing Mg(OH)₂ nanowaste. *Angew Chem Int Ed* 47:5619–5622
- McMullan G, Meehan C, Conneely A, Kirby N, Robinson T, Nigam P, Banat IM, Marchant R, Smyth WF (2001) Microbial decolorisation and degradation of textile dyes. *Appl Microbiol Biotechnol* 56:81–87
- Monson PD, Ankley GT, Kosian PA (1995) Phototoxic response of *Iuribacillus-variegatus* to sediments contaminated by polycyclic aromatic-hydrocarbons. *Environ Toxicol Chem* 14:891–894
- Mustafa T, Demirhan C, Mustafa S (2008) 5-Chloro-2-hydroxyaniline-copper (II) coprecipitation system for preconcentration and separation of lead and chromium at trace levels. *J Hazard Mater* 158:137–141
- Ng DKS, Foo DCY, Tan RR (2007) Targeting for total water network, waste stream identification. *Ind Eng Chem Res* 46:9107–9113
- Pandit P, Basu S (2004) Removal of ionic dyes from water by solvent extraction using reverse micelles. *Environ Sci Technol* 38:2435–2442
- Qu XL, Wang XR, Zhu DQ (2007) The partitioning of PAHs to egg phospholipids facilitated by copper and proton binding via cation- π interactions. *Environ Sci Technol* 41:8321–8327
- Robinson T, McMullan G, Marchant R, Poonam N (2001) Remediation of dyes in textile effluent: a critical review on current treatment technologies with a proposed alternative. *Bioresour Technol* 77:247–255
- Sathe TR, Agrawal A, Nie SM (2006) Mesoporous silica beads included with semiconductor quantum dots and iron oxide nanocrystals: dual-function microcarriers for optical encoding and magnetic separation. *Anal Chem* 78:5627–5632
- Schenker U, Scheringer M, Hungerbühler K (2007) Including degradation products of persistent organic pollutants in a global multi-media box model. *Environ Sci Pollut Res* 14:145–152
- Schur M, Bems B, Dassenoy A, Kassatkine I, Urban J, Wilmes H, Hinrichsen O, Muhler M, Schlögl R (2003) Continuous coprecipitation of catalysts in a micromixer: nanostructured Cu/ZnO composite for the synthesis of methanol. *Angew Chem Int Ed* 42:3815–3817
- Sourisseau C (2004) Polarization measurements in macro- and micro-raman spectroscopies: molecular orientations in thin films and azo-dye containing polymer systems. *Chem Rev* 104:3851–3891
- Takahashi Y, Kasai H, Nakanishi H, Suzuki TM (2006) Test strips for heavy-metal ions fabricated from nanosized dye compounds. *Angew Chem Int Ed* 45:913–916
- Tal A (2006) Seeking sustainability: Israel's evolving water management strategy. *Science* 313:1081–1084
- Talarposhti AM, Donnelly T, Anderson GK (2001) Colour removal from a simulated dye wastewater using a two-phase anaerobic packed bed reactor. *Water Res* 35:425–432
- Ugurlu M, Kula O (2007) Decolorization and removal of some organic compounds from olive mill wastewater by advanced oxidation processes and lime treatment. *Environ Sci Pollut Res* 14:319–325
- Vijayaraghavan K, Yun YS (2008) Bacterial bioadsorbents and biosorption. *Biotechnol Adv* 26:266–291
- Wisian-Neilson P (2003) Polymer films with included metal nanoparticles. Springer series in materials science. *J Am Chem Soc* 125:6338–6339
- Xing B, Pan B, Ning P (2008) Part IV—sorption of hydrophobic organic contaminants. *Environ Sci Pollut Res* 15:554–564
- Yang M, Yu JW, Li ZL, Guo ZH, Burch M, Lin TF (2008) Taihu lake not to blame for Wuxi's woes. *Science* 319:158a
- Zhang QF, Chou TP, Russo B, Jenekhe SA, Cao GZ (2008) Aggregation of ZnO nanocrystallites for high conversion efficiency in dye-sensitized solar cells. *Angew Chem Int Ed* 47:2402–2406